IMPERIAL COLLEGE OF SCIENCE AND TECHNOLOGY

Department of Aeronautics, London SW7 2BY, England

Progress report on contract NAGW-581 "Burst Vortex / Boundary Layer Interaction", 1 Sept. 1987 - 29 Feb. 1988

P. Bradshaw, Principal Investigator; M. Naaseri, Research Assistant

Summmary

Work on this new contract has proceeded on schedule, as outlined in the Proposal. Several configurations of delta-wing vortex generator and boundary-layer test plate have been tested, and two final ones selected. This progress report includes sample measurements and flow visualizations in the candidate configurations, together with more detailed measurements in one of the two "final" arrangements - which have been carefully selected so that a pure vortex bursts repeatably and then interacts, in as simple a fashion as possible, with a simple turbulent boundary layer.

A significant feature of the work, not immediately apparent from the literature, is that different intensities of bursting or breakdown, like different strengths of shock wave or hydraulic jump, can be produced by minor changes of configuration: the weaker breakdowns do not produce flow reversal. The initial measurements have been done with a fairly weak, but repeatable, breakdown: basic measurements on the second "final" arrangement, with a stronger breakdown, are in progress.

Introduction

This study is a successor to that done under NAGW-581 "Vortex / Boundary-Layer Interactions" (the final report by Cutler and Bradshaw - Ref. 1, submitted in Sept. 1987 - presents full details of mean-flow and turbulence measurements, intended to serve as test cases for code validation or development). In that study, a trailing vortex pair from a delta wing passed over the top of a horizontal test plate, with its span parallel to that of the delta wing: a typical test configuration is shown in Fig. 1. The small vertical separation of the delta wing and the test plate ensured that most of the non-rolled-up part of the delta wing wake passed under the test plate. The delta wing vortices diverged in the spanwise direction under the influence of their own induced velocity and that due to the image vortices below the plate, so that the interactions between each vortex and the plate boundary layer were virtually independent, except that the boundary layer near the test-plate centre line suffered the effects of strong lateral divergence.

The present extension of Cutler and Bradshaw's work is intended to study the interaction of a burst vortex and a boundary layer: it is not expected that there will be major qualitative differences from the earlier case, but study of a burst-vortex / boundary-layer interaction is a necessary preliminary to work on a burst-vortex / separated-flow interaction. The tunnel and instrumentation are the same, and the main difference is in the detailed configuration of the test rig. The simplest way to burst a vortex is to apply an adverse pressure gradient, which we finally chose to do by inclining the test plate and / or the tunnel roof: several adequate methods of calculating turbulent boundary layers in adverse pressure gradient already exist, and certainly any prediction method capable of handling vortex interactions could also handle boundary layers in pressure gradients.

Vortex "breakdown" or "bursting" is a simple physical phenomenon, much confused

by mathematicians. A simple explanation (by a mathematician!) is in Ref. 2, pp. 550-555:

(i) if a vortex undergoes longitudinal deceleration, its radius increases as a result of mass conservation;

(ii) as a result of angular-momentum conservation, the angular velocity Ω at given radius r decreases;

(iii) as a result of the radial momentum equation, which reduces to $\partial p/\partial r = \rho r\Omega^2$, the pressure near the axis increases;

(iv) as a result of positive $\partial p/\partial x$ near the axis, the vortex undergoes longitudinal deceleration;

GOTO (i).

Above a certain ratio of circumferential velocity to axial velocity, runaway instability results, possibly but not necessarily leading to reversed flow on the vortex core. In a flow confined by an aircraft wing or tunnel walls, the burst induced by this unstable feedback loop may not be as violent as in unrestricted flow, where axisymmetric or spiral recirculation can occur. In the present cases, the vortex is strongly constrained by the flat plate beneath it, with some effect of the wind tunnel walls; therefore, although the burst is well-defined, the axial velocity in the vortex downstream of breakdown is still positive everywhere.

Choice of Configuration

In the early stages of the present work, we verified our expectation that the symmetrical configuration of Cutler and Bradshaw (Fig. 1), in which we demonstrated vortex breakdown during a visit by Dr D.J. Peake, would not be suitable for detailed study: the rapid growth of the two vortices downstream of breakdown would result in interaction

between them. We therefore studied various geometries with the span of the delta wing vertical, so that only one vortex passed over the horizontal test plate. An arrangement with the delta wing mounted wholly above, and in front of, the test plate ensured that one vortex would rapidly descend towards the test plate in the mutual induced velocity field which causes trailing vortices to move apart: however the non-rolled-up part of the delta-wing wake (essentially the part shed from the trailing edge) gradually fed into the rolled-up vortex and complicated the flow. We finally chose the vortex-generator configuration shown in Fig. 2, in which the delta wing was mounted *below* the test plate, so that only one vortex passed above the test plate. This removed most of the non-rolled-up part of the vortex, and also a small segment of the vortex proper (Fig. 5(a)), but had the disadvantage that the vortex moved upward, and thus away from the plate, in the induced velocity field.

The simplest perturbation that initiates a breakdown is an externally-imposed adverse pressure gradient. We began by imposing a short region of adverse pressure gradient, by applying suction to the tunnel roof to produce a monotonic pressure rise (Fig. 2(a): in a blower tunnel like that used here, such suction can be applied very easily by opening the roof of the tunnel and obstructing the exit). The disadvantage was that the vortex itself moved towards the roof, so that it did not spread into the boundary layer until too far down the working section. We next added a streamlined "bump" (Fig. 2(b)) to the tunnel roof, so as to induce an adverse pressure gradient followed by a favourable one, without a net upward deflection of the flow. However for constructional reasons it was difficult to trigger bursting at the right place in the tunnel. In principle, such concentrated regions of pressure rise should be the optimum for triggering stable vortex breakdown (we laid great stress on stability / repeatability and on insensitivity to the insertion of probes). However, after testing both a bump and a region of suction, we finally chose to stabilize

vortex breakdown by a prolonged adverse pressure gradient, induced by inclining the test plate at a positive angle of incidence; the burst vortex spread sufficiently rapidly that it intersected the test boundary layer within the working section, despite the upward induced velocity enforced by the delta-wing vortex generator. The burst was of the same mild character, with rapid change of growth rate but without recirculation, in all cases: that is, the vortices in the prolonged adverse pressure gradient do genuinely burst, rather than just spreading faster as the flow decelerates. Our two final configurations, therefore, feature a vertical-span delta wing (span 7 in $\equiv$ 178 mm, aspect ratio 1.0, incidence 20 deg.), mounted ahead of and below a test plate inclined at 1.82 deg. positive incidence so that one of the tip vortices bursts in the adverse pressure gradient above the test plate and thereafter spreads into the test-plate boundary layer. Fig. 2(c) shows a configuration with the tunnel roof horizontal. To produce a stronger adverse pressure gradient and thus a stronger breakdown, the tunnel roof was inclined upwards, at 3.18 deg., starting 25 in behind the leading edge of the plate (Fig. 2(d)).

We have carefully checked that the breakdown is repeatable from day to day. Also we found that our standard pitot- and hot-wire probes do not significantly influence the flow in the vortex, unless inserted into in the breakdown region itself. (We did not at any stage intend to investigate the breakdown region as such, and our code-validation results will be presented with an initial measurement plane downstream of the breakdown, but upstream of the point where the vortex enters the boundary layer.)

Results Sept. 1987 - Feb. 1988

Figs. 2(a-d) show the various configurations tested as improvements on the unburst-vortex configuration of Cutler and Bradshaw (Fig. 1). Briefly, the decisions were, whether to mount the delta wing with its span horizontally (as in Cutler & Bradshaw's work) or

vertically; and whether to induce an adverse pressure gradient by a bump on the roof, suction through the roof, or inclination of the roof and/or inclination of the test plate. As indicated above, the final choice was a vertical-span delta wing and an inclined test plate (case "C", weak breakdown) or an inclined plate and tunnel roof (case "D", strong breakdown). We do not regard this as the only possible configuration, and therefore include details of the rejected geometries.

The initial investigations were done by piecemeal flow visualization and pitot measurements. Recently we have repeated the visualization, to produce the photographs of each configuration shown in Fig. 3.

Qunatitative work has been interrupted by unserviceability of the data-logging computer (a 1983-vintage PCAT precursor, now replaced): however a fair aggregate of data has been obtained, including total-pressure measurements in configurations "C" and "D" and preliminary hot-wire measurements.

Fig.4 shows total-pressure contours in configuration "C", and Fig. 5 shows a colour-map version of Fig. 4(e), at low resolution for illustrative purposes. (Our usual procedure is to present colour-graphics plots for easy eyeballing, with detailed data in machine-readable form for archive purposes.) The results given here were obtained from pitot tubes aligned with the x axis, but our checks have shown that reductions in measured total pressure due to yaw or pitch of the flow are small within the range of the present experiments, so that these results should be definitive.

Discussion

The smoke-flow pictures in Fig. 3, which were all taken at long exposure to show up mean boundaries, do not show the breakdown of the vortex core as clearly as visual observation: the top view of configuration "C" (Fig. 3(c.9)) is about the clearest. The

general appearance is like laminar-turbulent transition, which indeed occurs: the quasi-laminar core of fluid in solid-body rotation (Ref. 1) diffuses rapidly as the angular velocity decreases (stage (ii), above) and the strong centrifugal destabilization decreases also. The turbulence in the outer part of the vortex does not change instantaneously, and the increase in spreading rate (Fig. 3(c.9)) results from streamline divergence in decelerating flow rather than from an immediate change in entrainment velocity.

In general, total pressure is more informative than velocity magnitude in flows with large static-pressure gradients: a simple transformation of the boundary-layer equations equates the streamwise gradient of total pressure to the lateral / radial gradient of Reynolds shear stress. However, vortex breakdown, whose main consequence is a rapid rise in *static* pressure on the axis, does not lead to an equally rapid change in total pressure, and so the present total-pressure results (Fig. 4) do not show up the breakdown very spectacularly. It is very difficult to measure static pressure within a vortex with any assurance of accuracy, because mean and fluctuating inclinations of the flow strongly affect the readings: we intend to measure the mean velocity components with hot wires, so that static pressure can be deduced as the difference between total pressure and dynamic pressure. The total-pressure measurements do confirm and amplify the smoke-flow pictures, and show how the boundary layer is distorted by the vortex.

Future plans (see also separate renewal proposal)

In the rest of the contract year we will start acquiring hot-wire data for the two chosen vortex / plate configurations. Even with modern micro-computer-based data logging equipment this is not a fast process, because of the need to check calibration drift, and the work will not be finished in the current year. Although turbulence modelling is not a specific part of the present contract, we hope to start interacting with modelling

work which is already in progress under an agreement with British Maritime Technology Ltd., and this interaction should begin shortly.

References

1. Cutler, A.D. and Bradshaw, P. Vortex/Boundary-layer interactions: data report. Final Report on NASA grant NAGW-581, Imperial College Aero TN 87-102, 1987.

2. Batchelor, G.K. *An Introduction to Fluid Dynamics.* University Press, Cambridge, 1967.

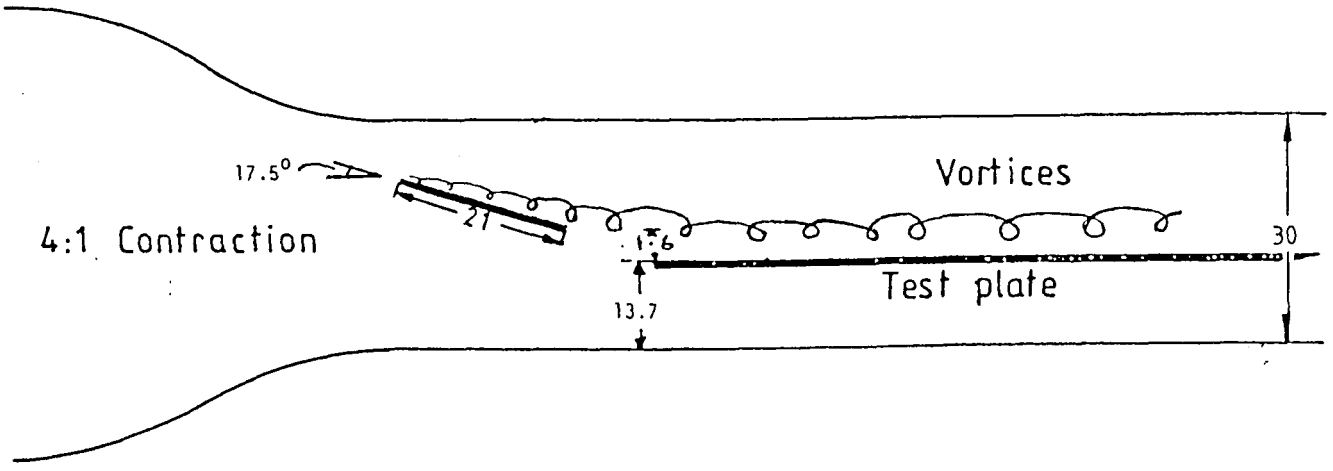

Dimensions in inches

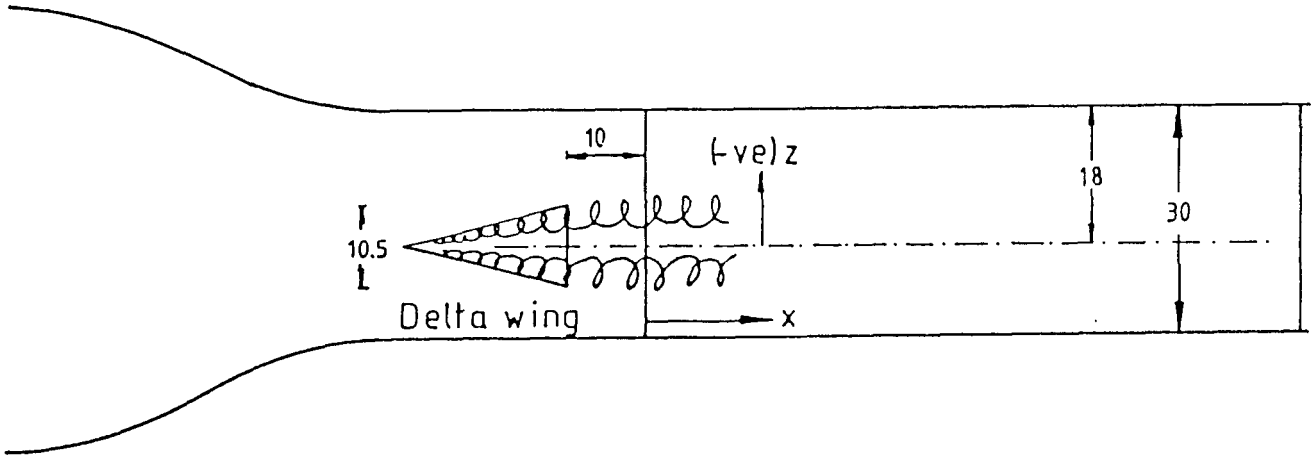

Fig. 1 Unburst-vortex configuration of Cutler and Bradshaw (Ref.1): all measurements in inches.

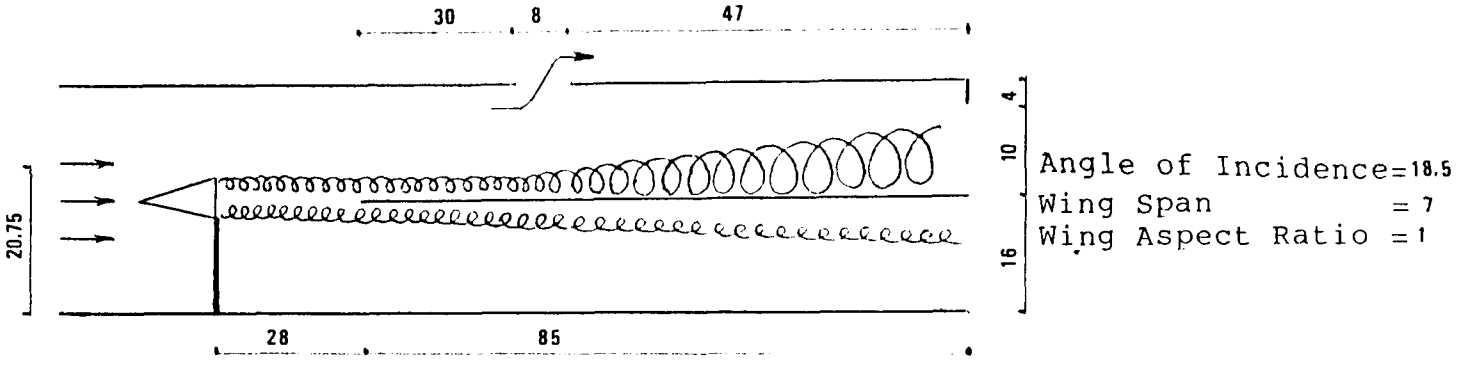

Fig. 2(a) - Configuration "A".

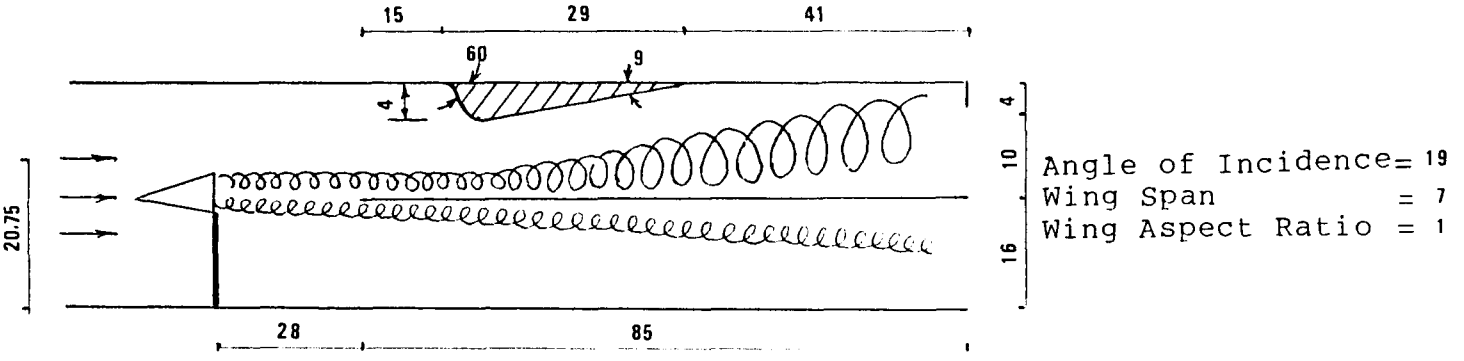

Fig. 2(b) - Configuration "B".

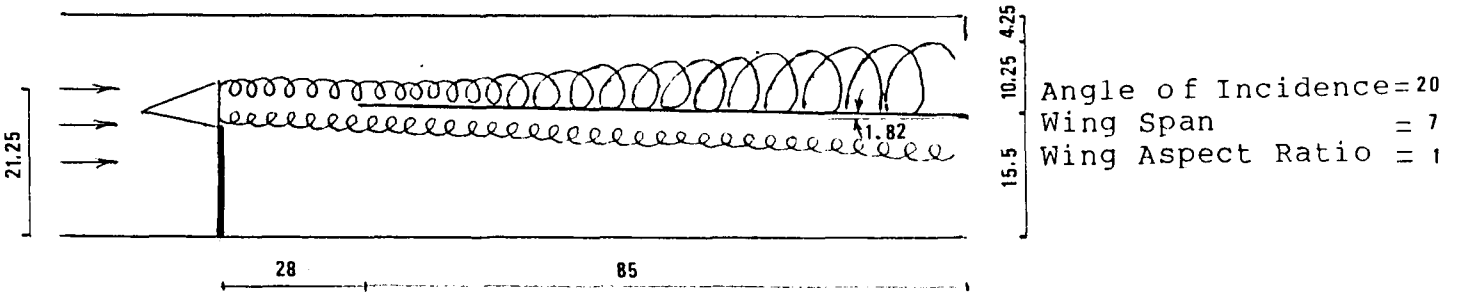

Fig. 2(c) - Configuration "C".

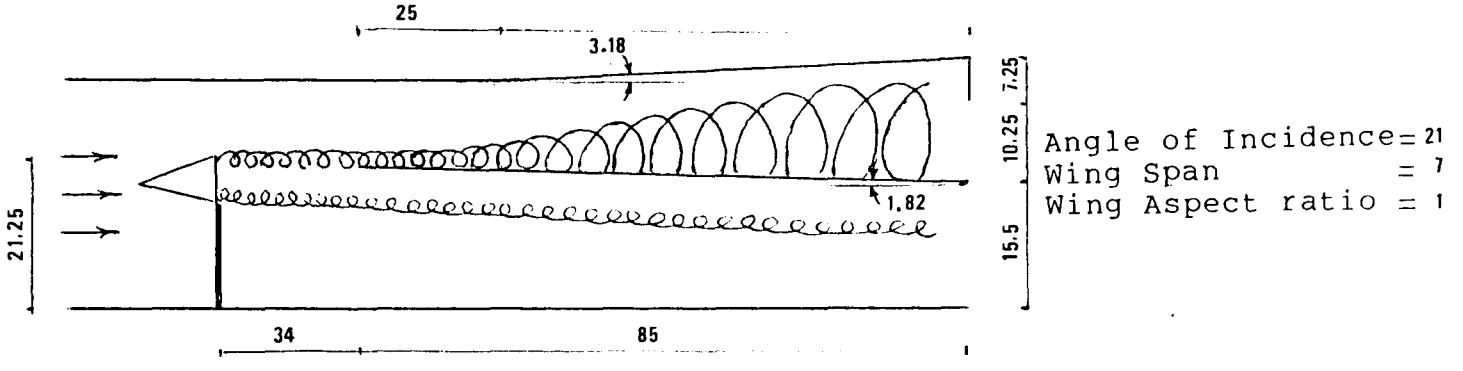

Fig. 2(d) - Configuration "D".

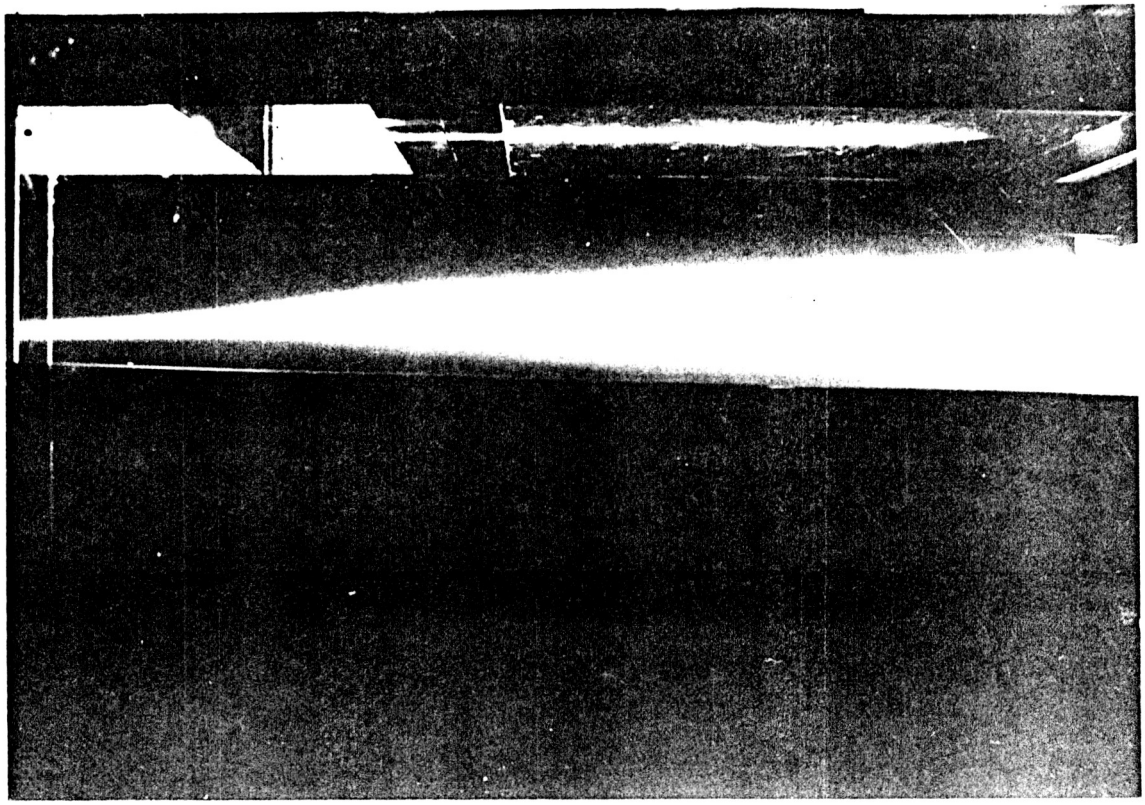

Fig. 3(a.1) - Long-exposure photograph of smoke-filled vortex: side view of configuration "A".

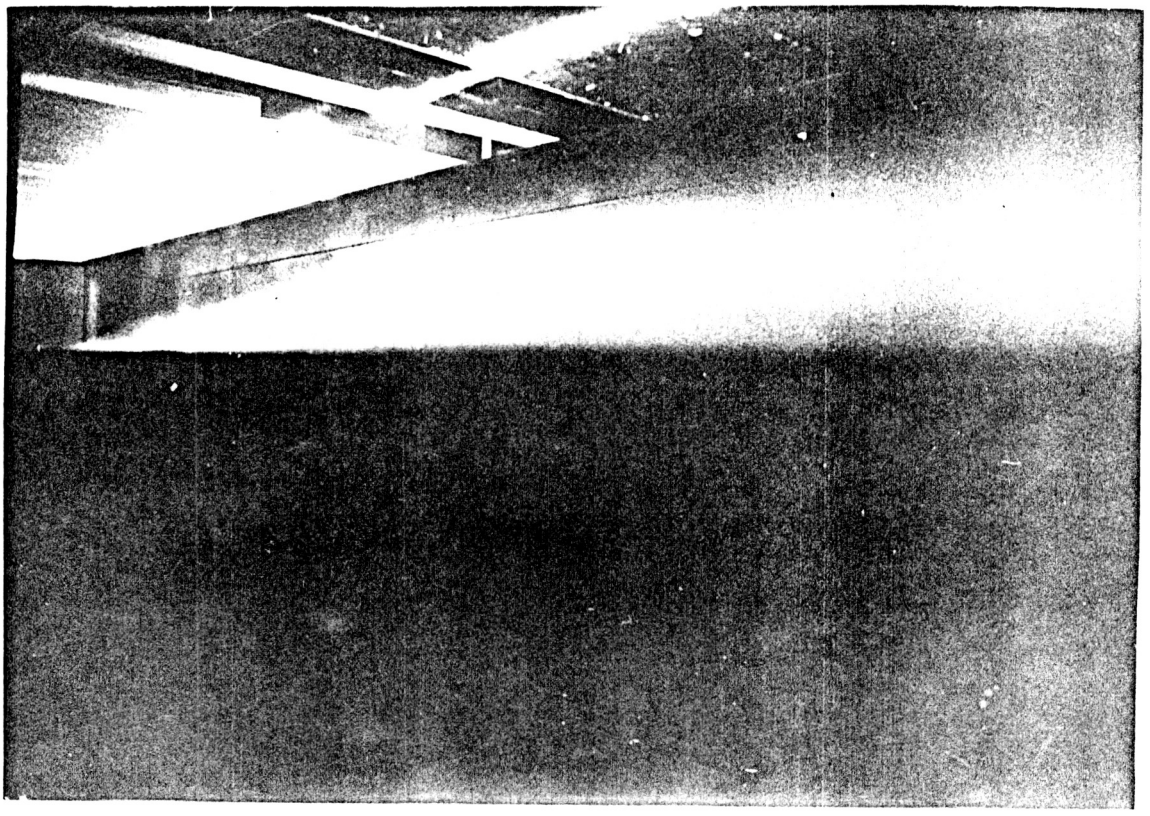

Fig. 3(a.2) - Back view of configuration "A".

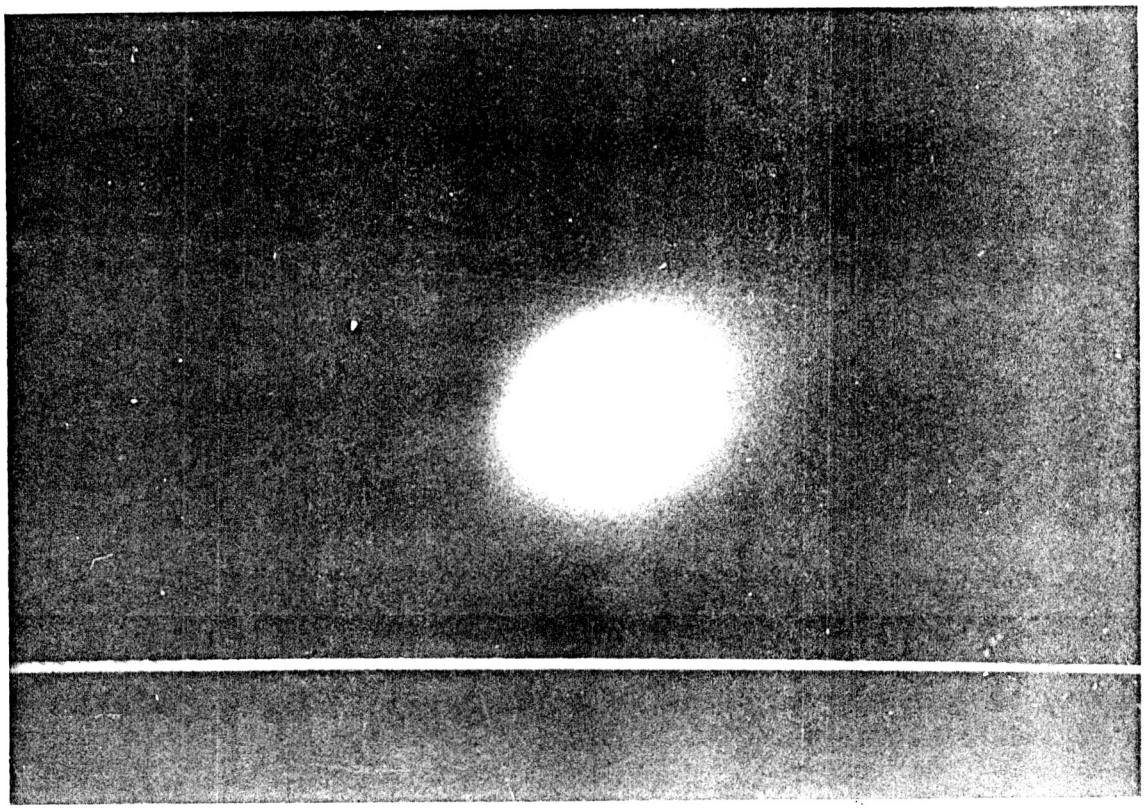

Fig. 3(a.3) - Cross-sectional view of "A", before burst, x = 15.0".

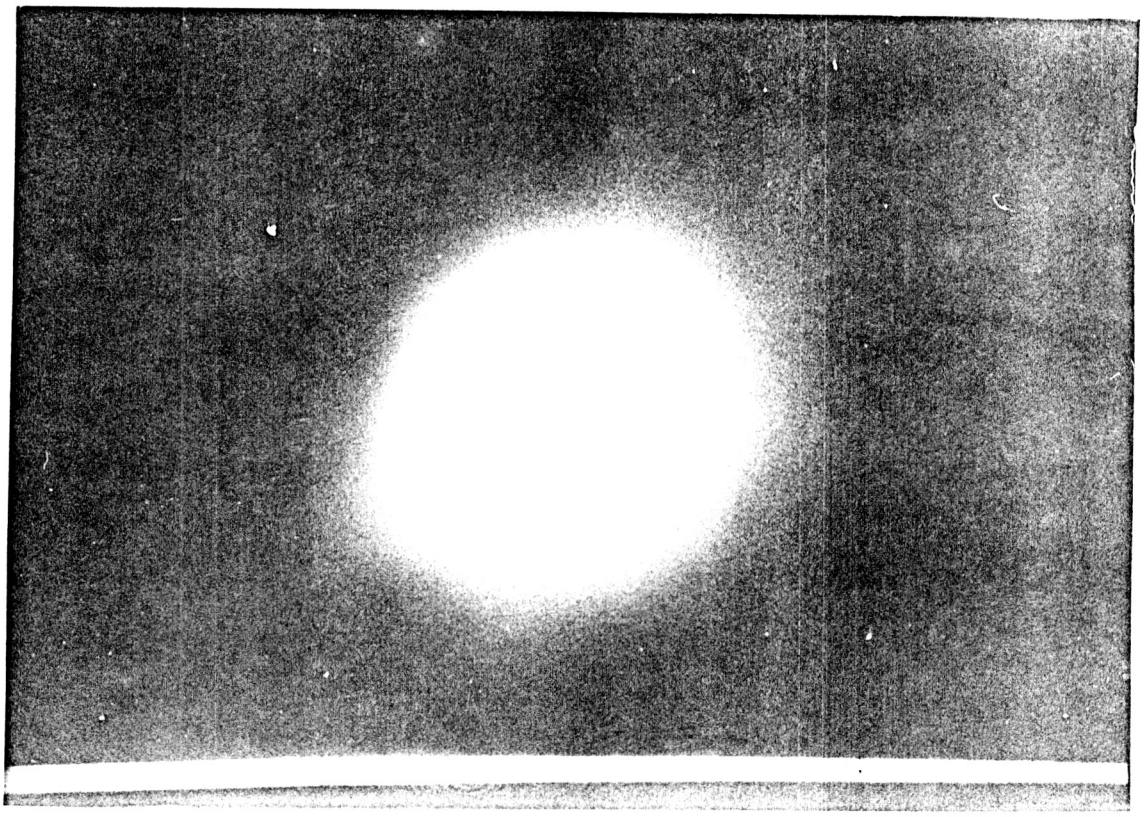

Fig. 3(a.4) - Cross-sectional view of "A", after burst, x = 32.5".

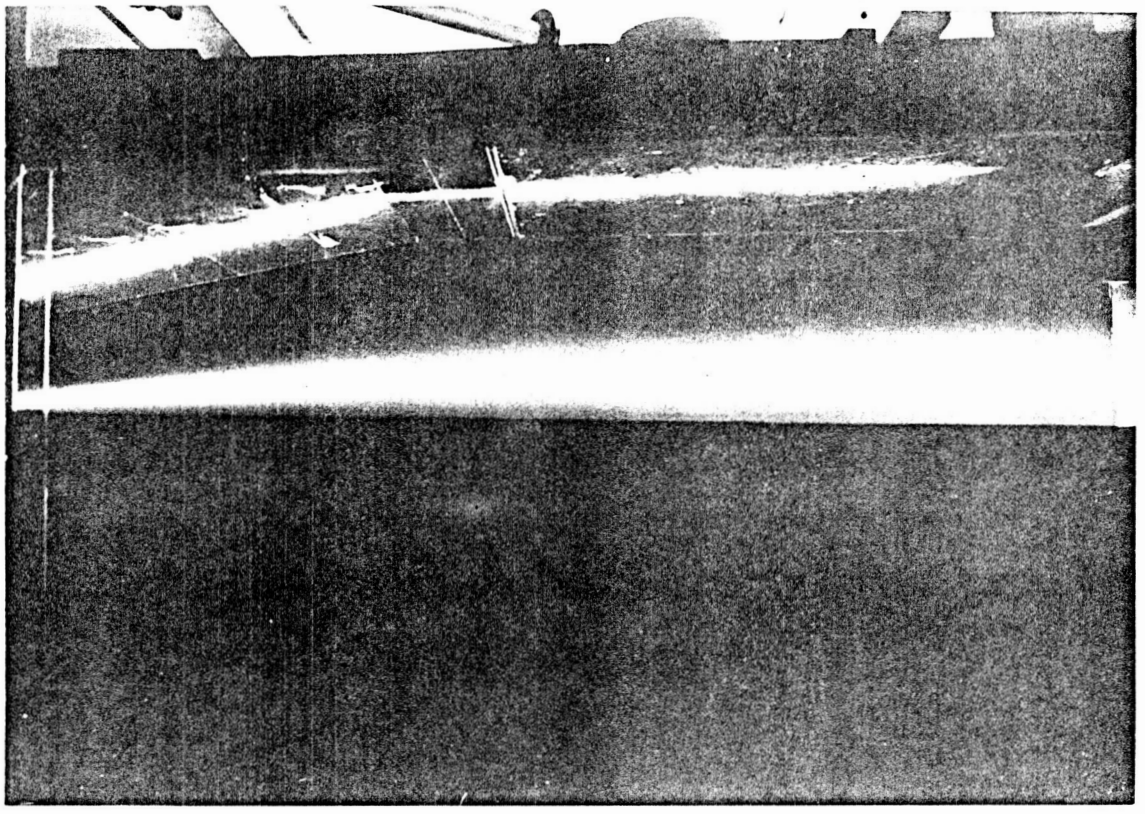

Fig. 3(b.1) - Side view of configuration "B".

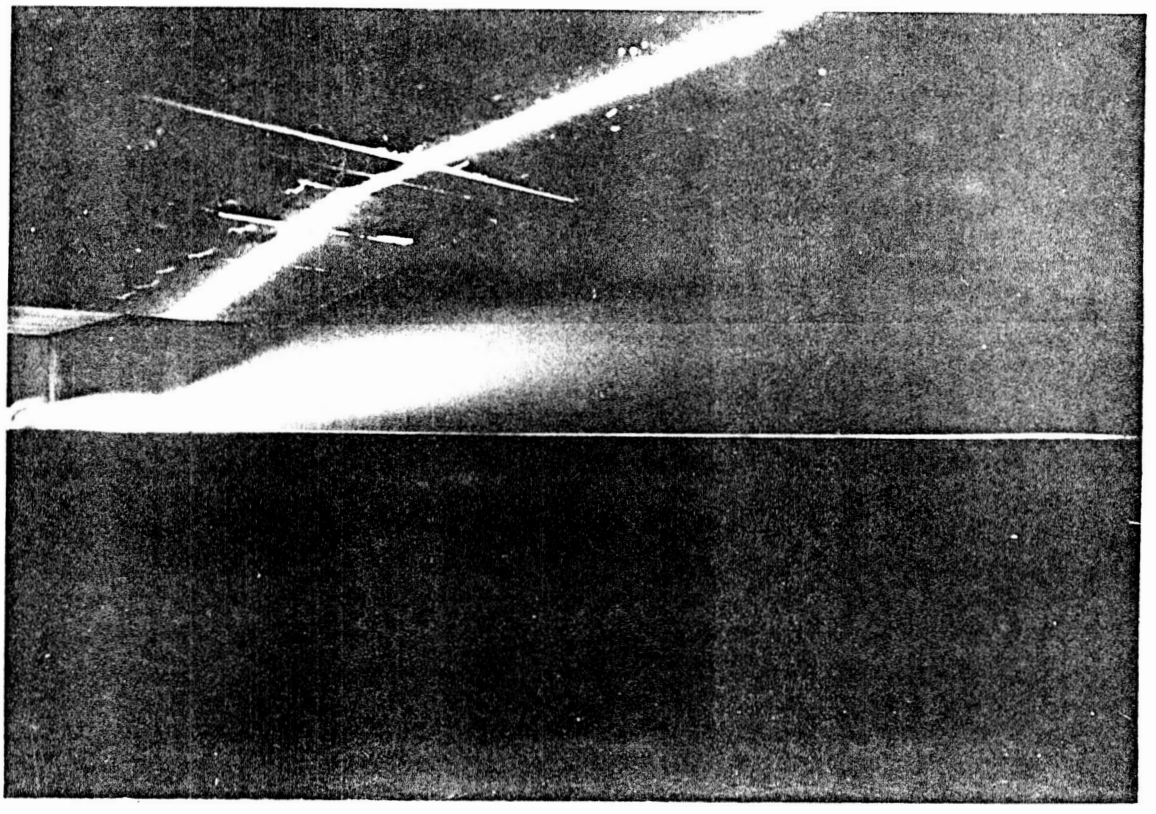

Fig. 3(b.2) - Back view of configuration "B".

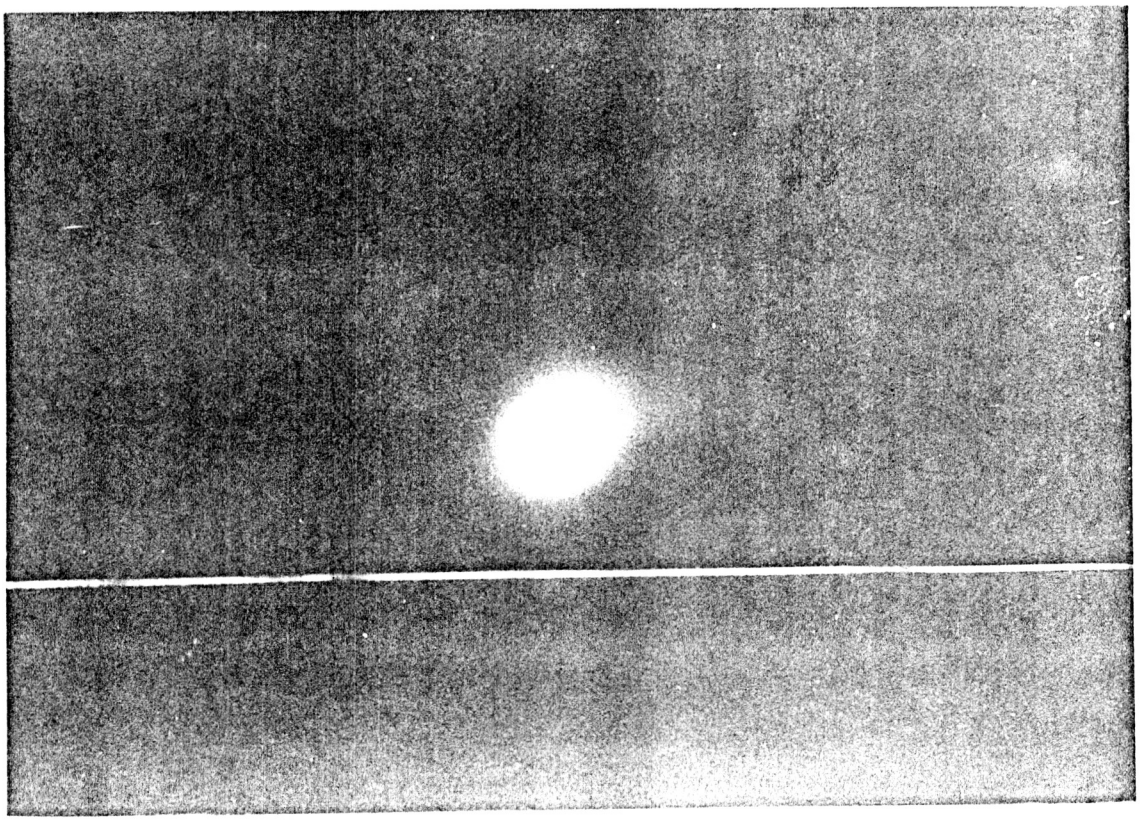

Fig. 3(b.3) - Cross-sectional view of "B", before burst, x = 15.0".

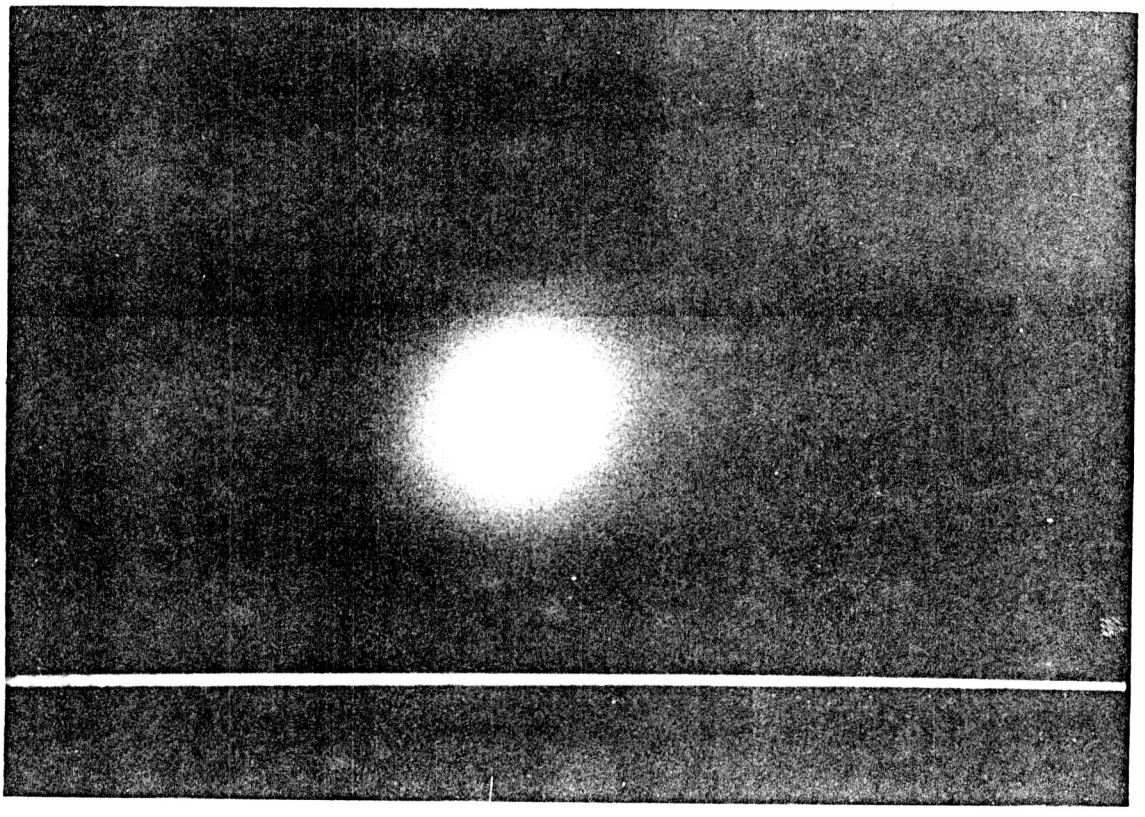

Fig. 3(b.4) - Cross-sectional view of "B", after burst, x = 32.5".

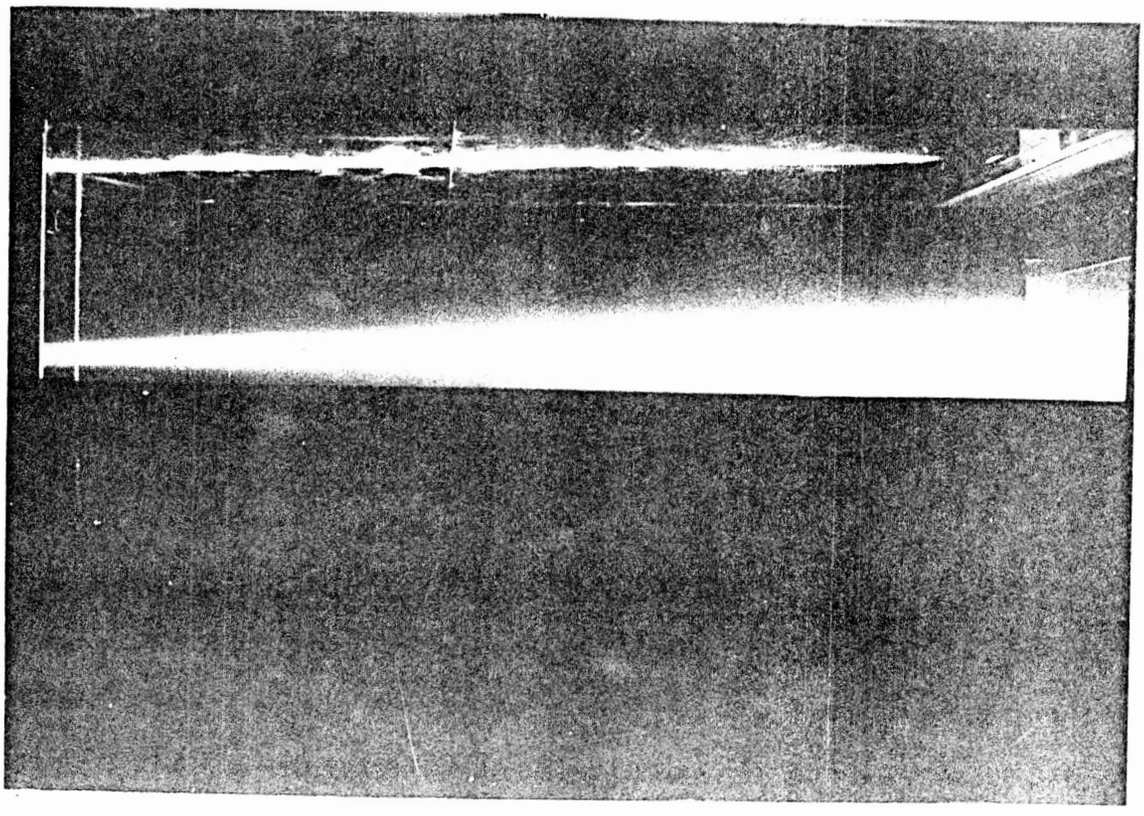

Fig. 3(c.1) - Side view of configuration "C".

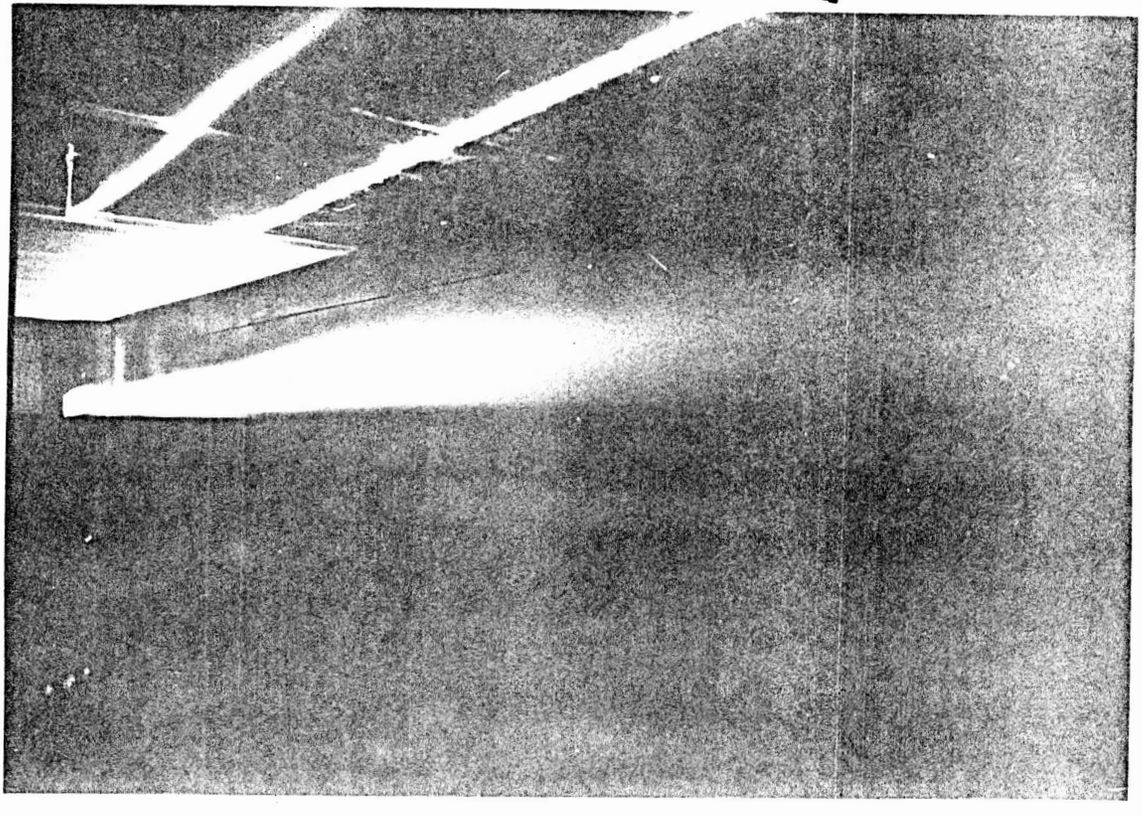

Fig. 3(c.2) - Back view of configuration "C".

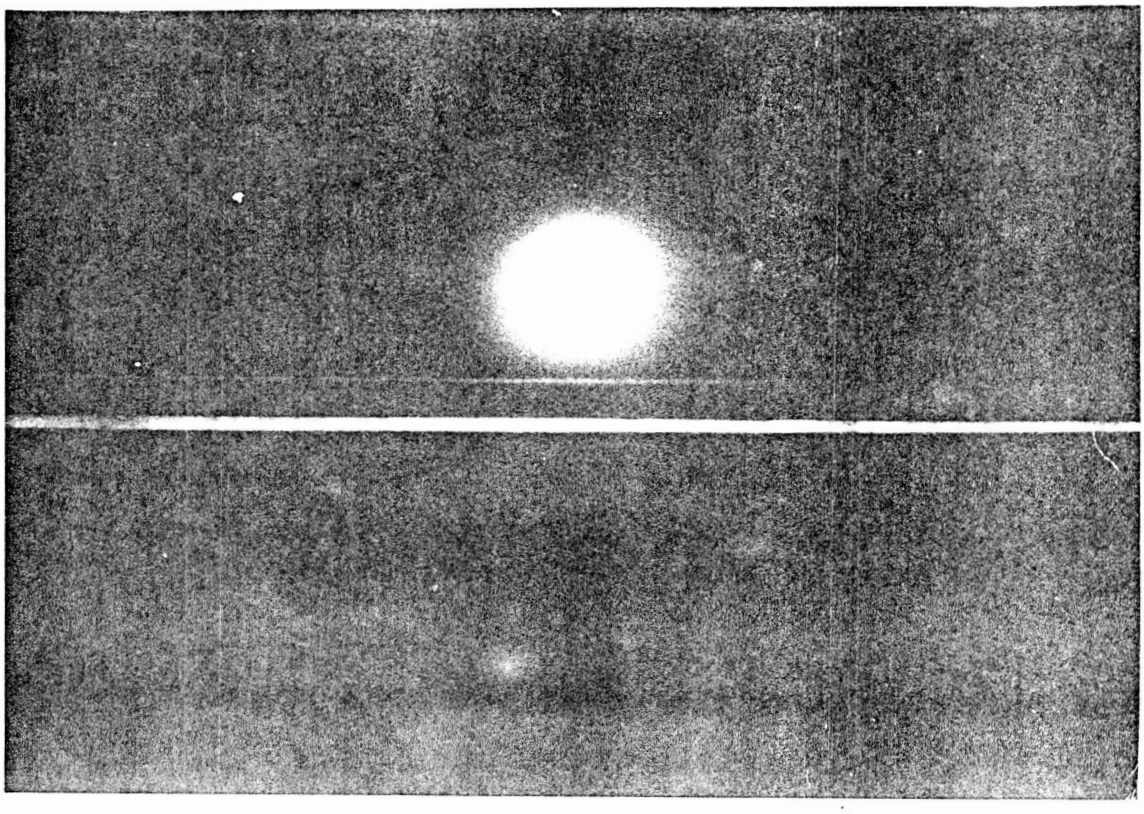

Fig. 3(c.3) - Cross-sectional view of "C", before burst, x = 1.5".

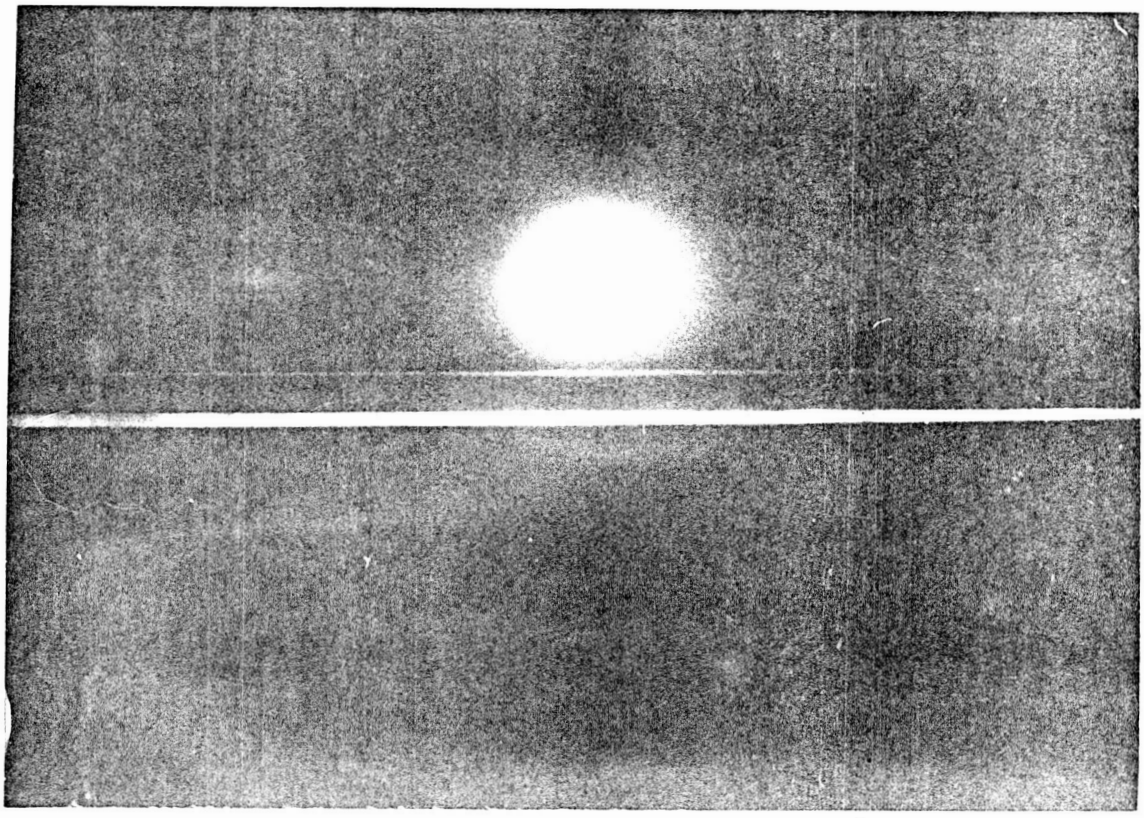

Fig. 3(c.4) - Cross-sectional view of "C", before burst, x = 15.0".

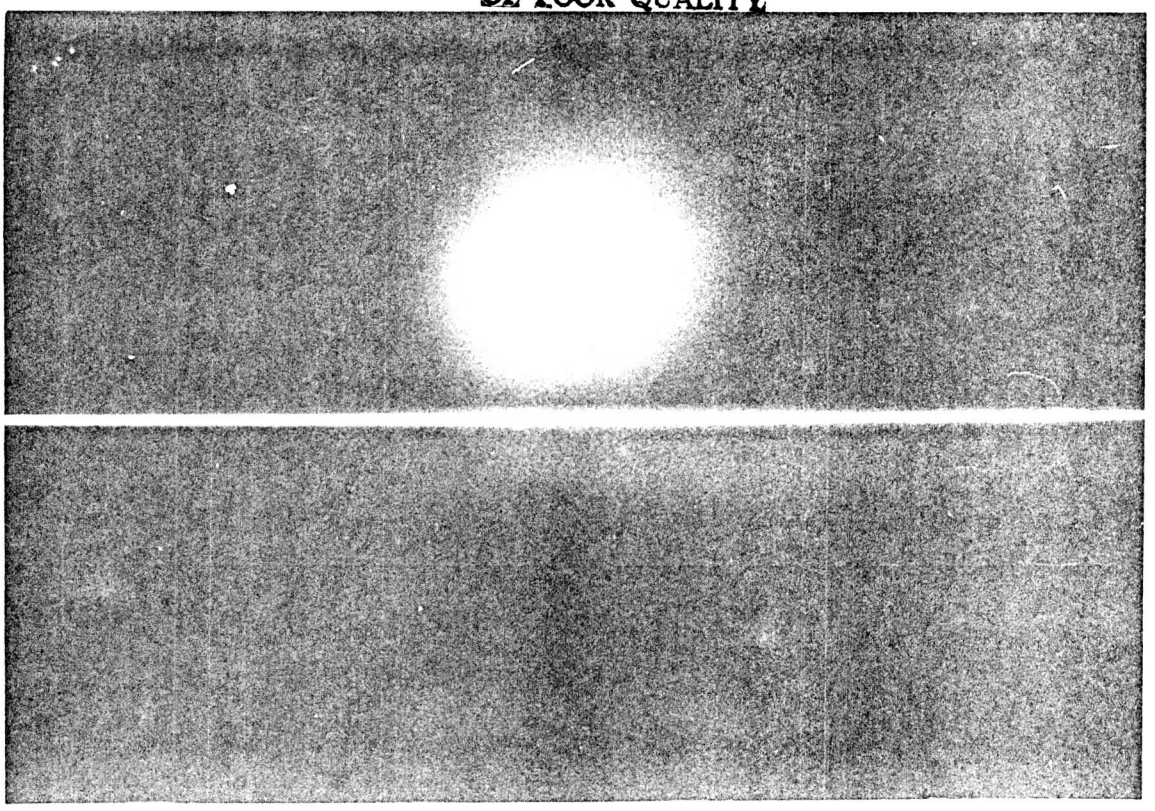

Fig. 3(c.5) - Cross-sectional view of "C", after burst, x = 32.5".

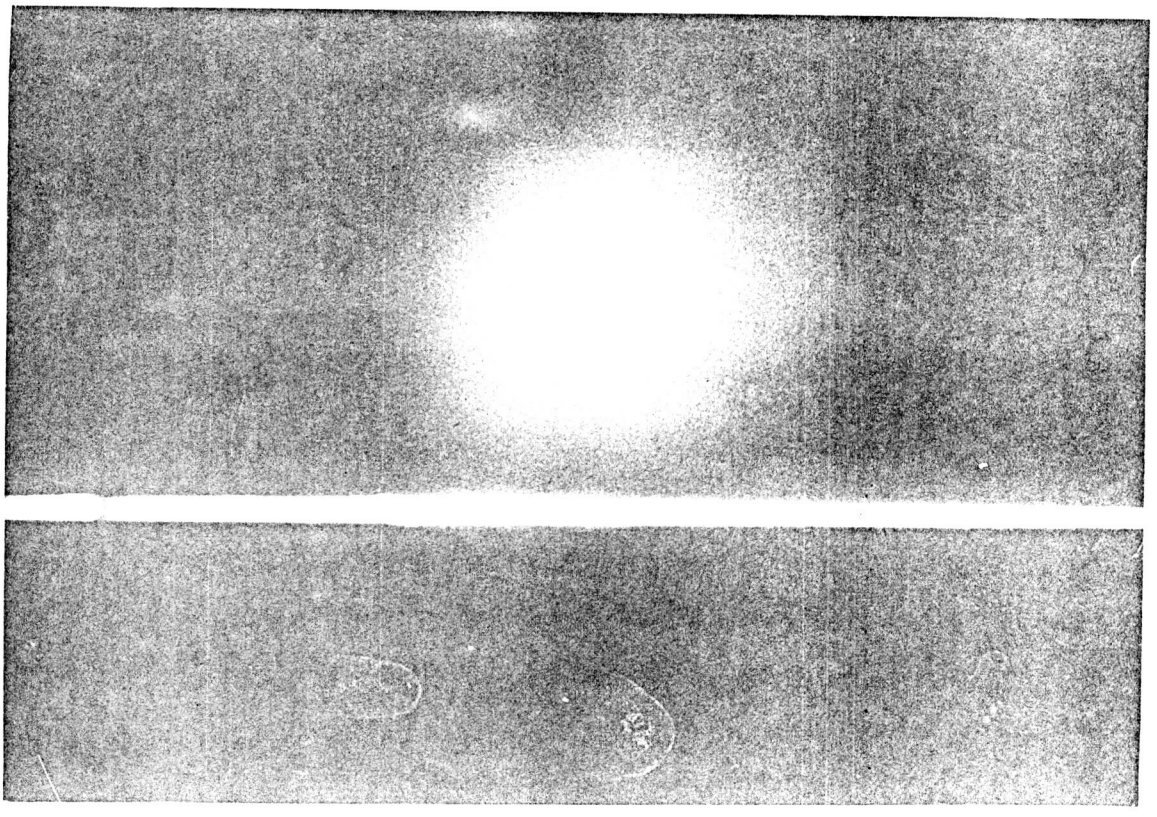

Fig. 3(c.6) - Cross-sectional view of "C", after burst, x = 42.5".

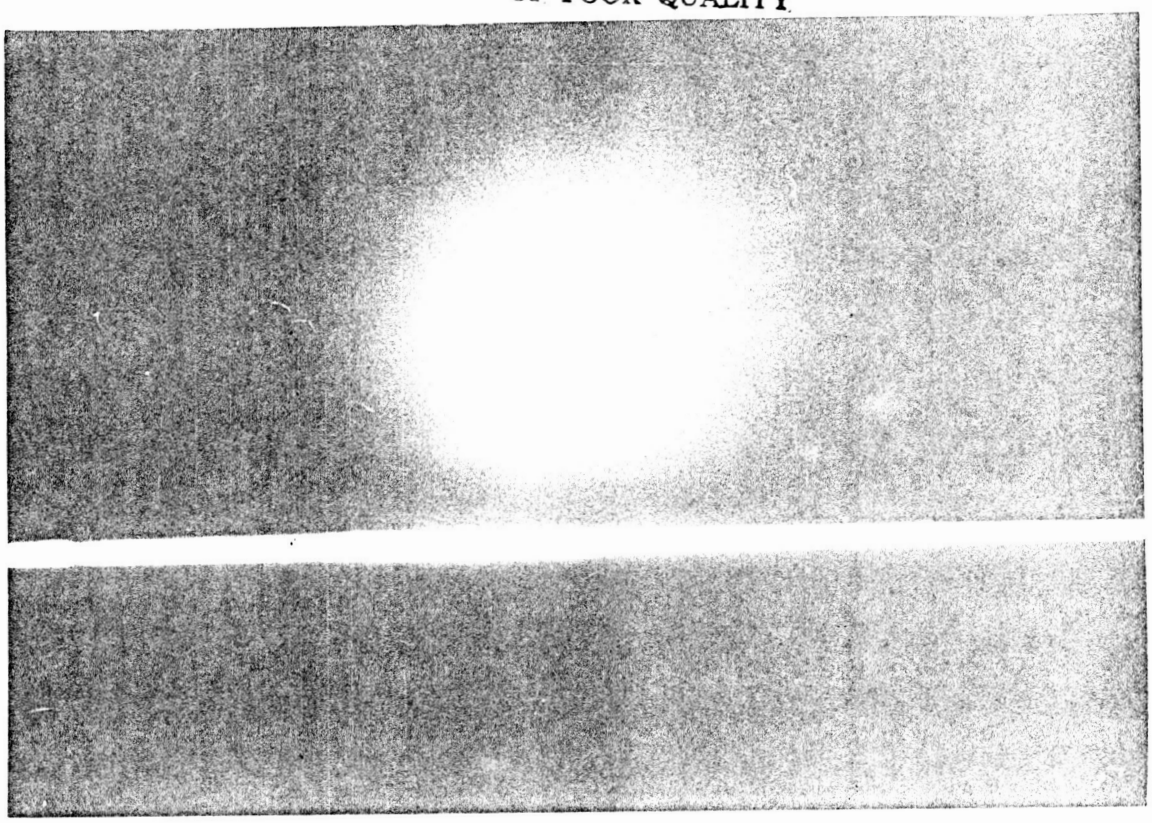

Fig. 3(c.7) - Cross-sectional view of "C", after burst, x = 52.5".

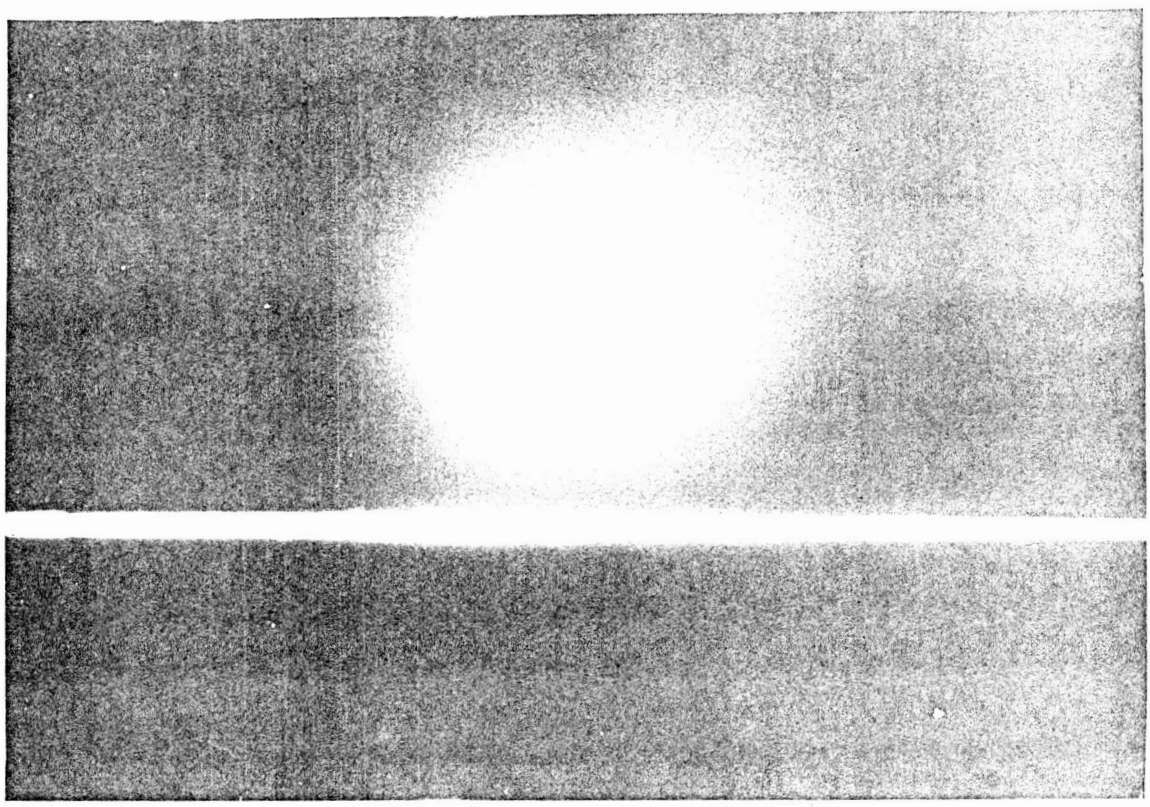

Fig. 3(c.8) - Cross-sectional view of "C", after burst, x = 62.5".

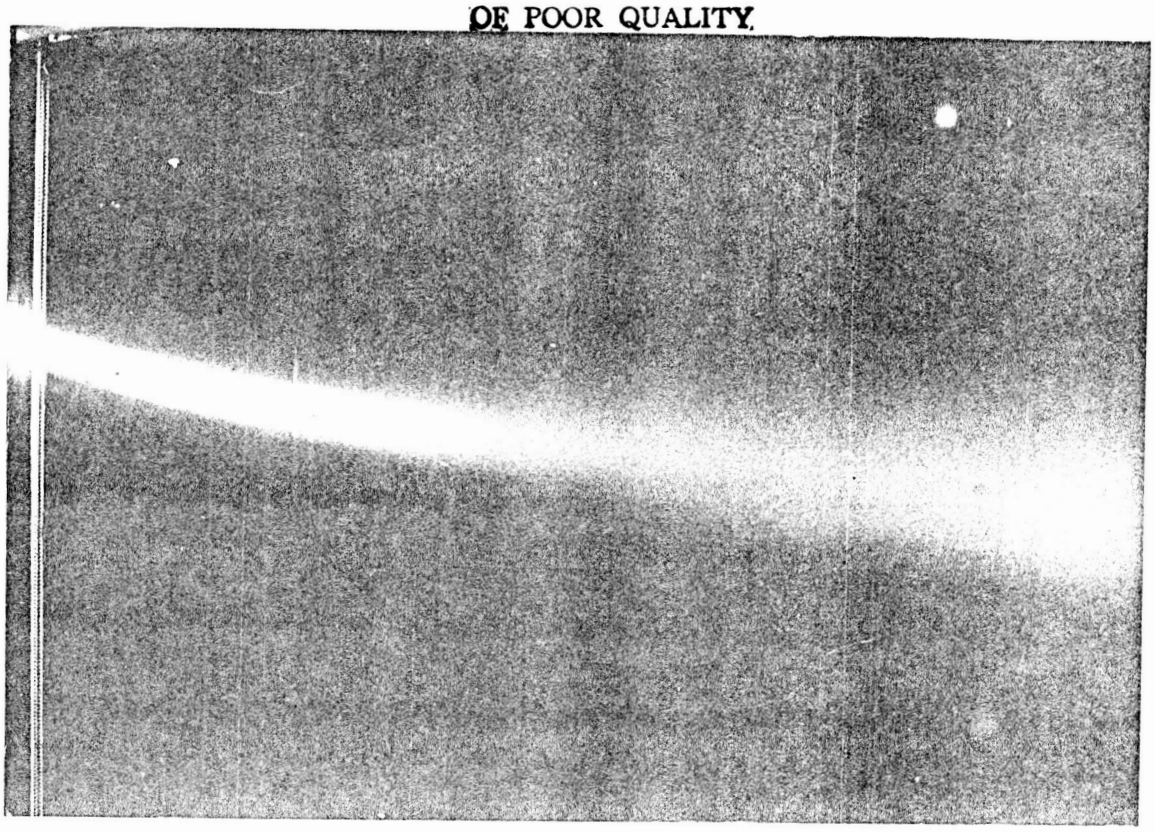

Fig. 3(c.9) - Top view of configuration "C".

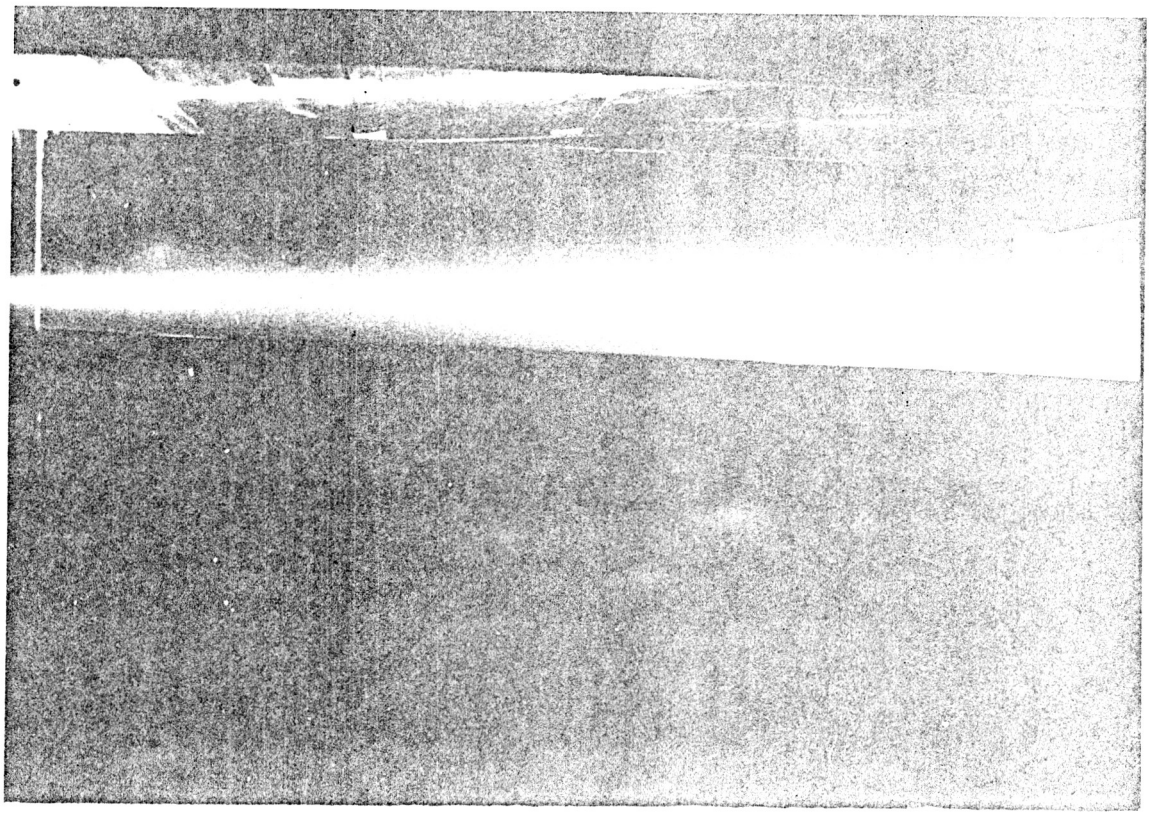

Fig. 3(d.1) - Side view of configuration "D".

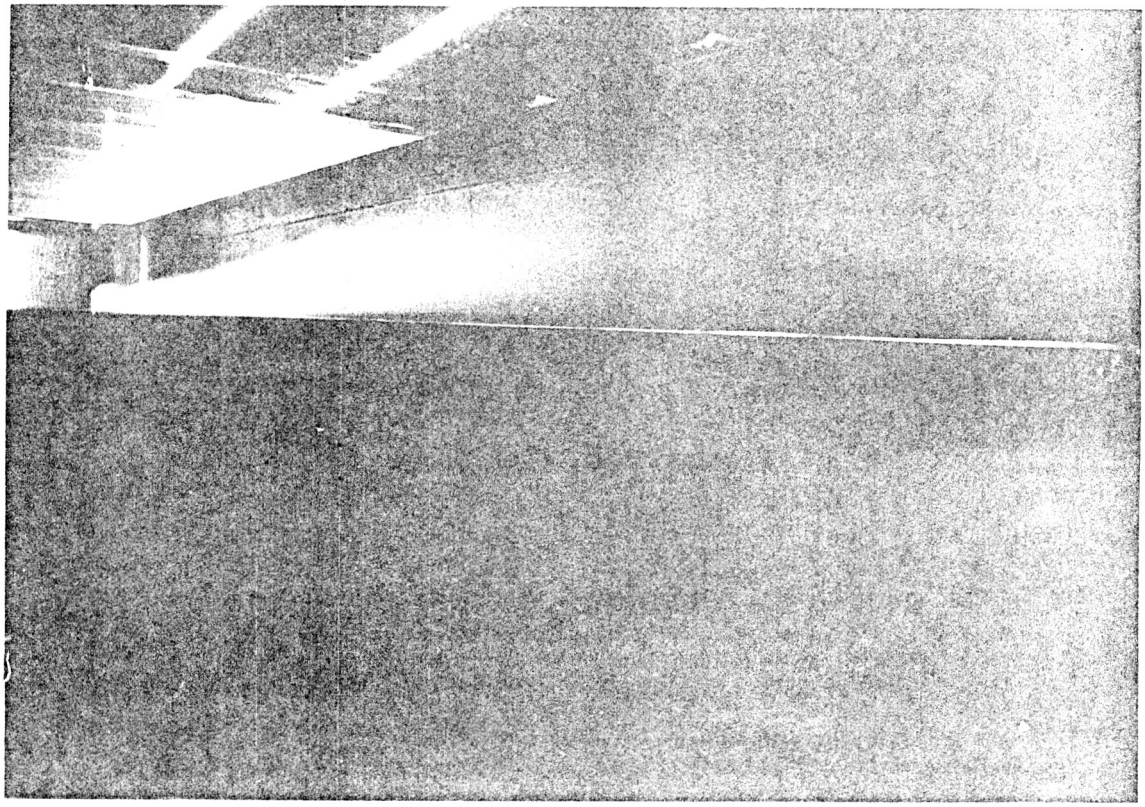

Fig. 3(d.2) - Back view of configuration "D".

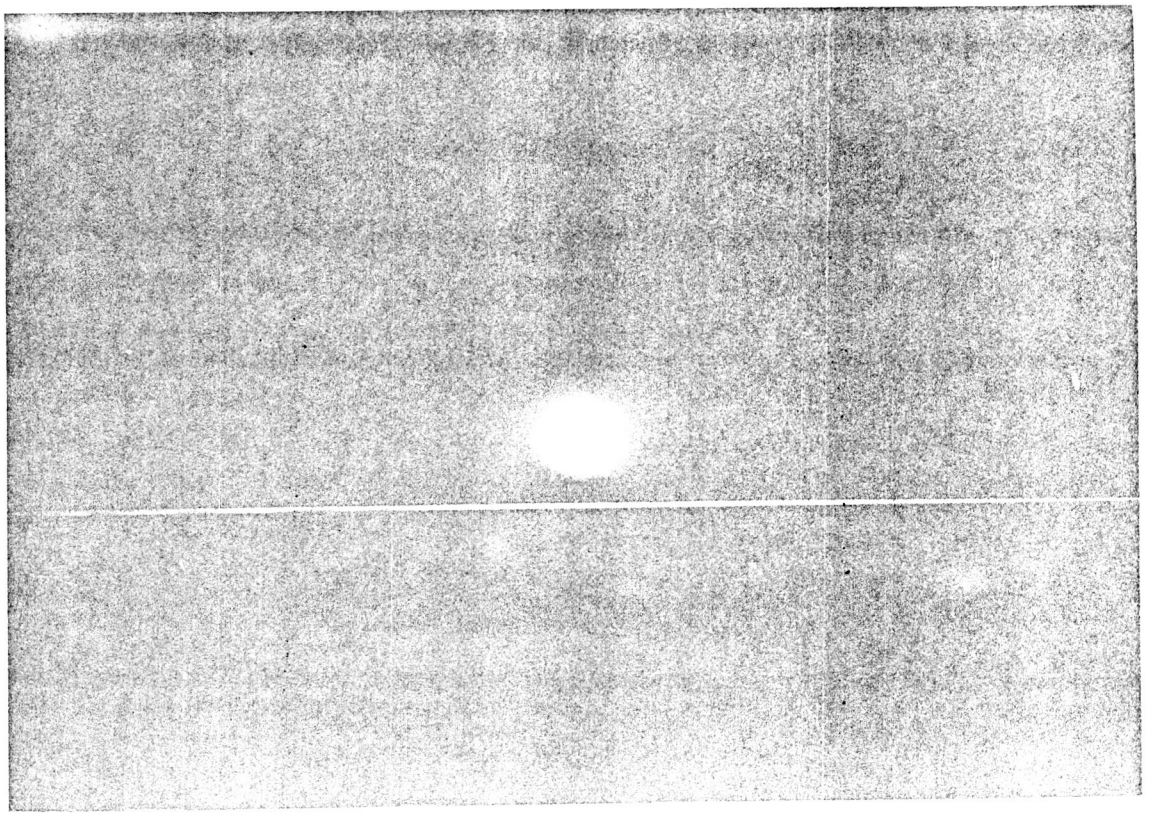

Fig. 3(d.3) - Cross-sectional view of "D", before burst, x = 10.0".

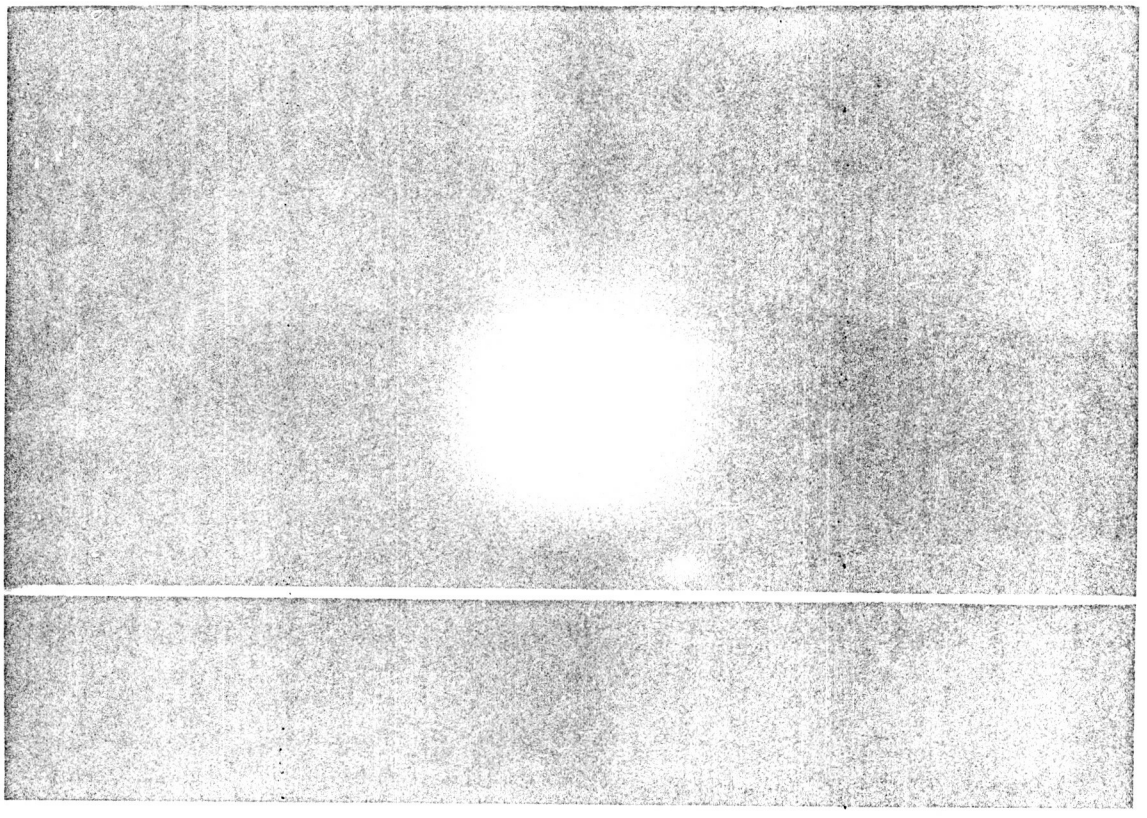

Fig. 3(d.4) - Cross-sectional view of "D", after burst, x = 32.5".

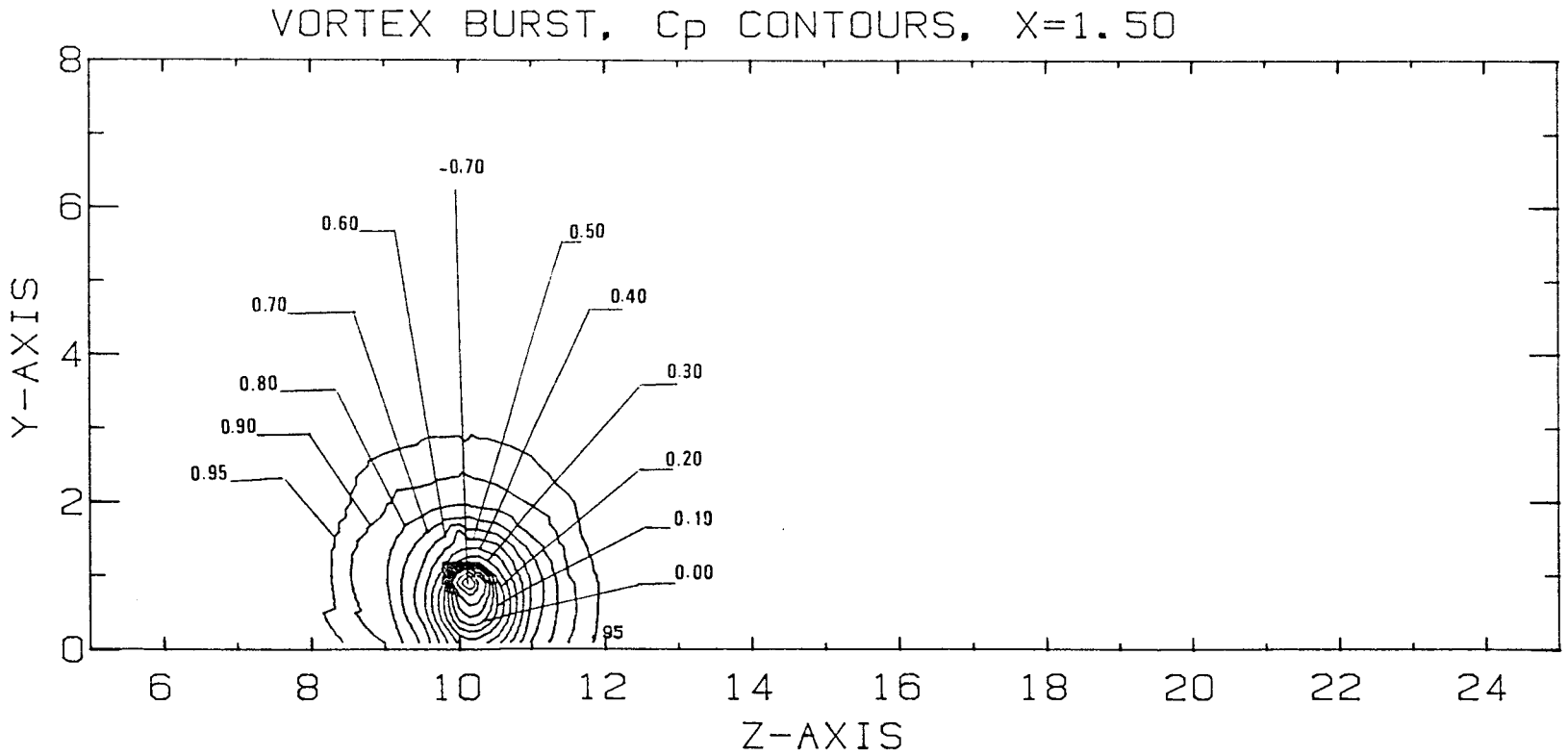

Fig. 4(a) - Total-pressure contours, configuration "C", x = 1.5".

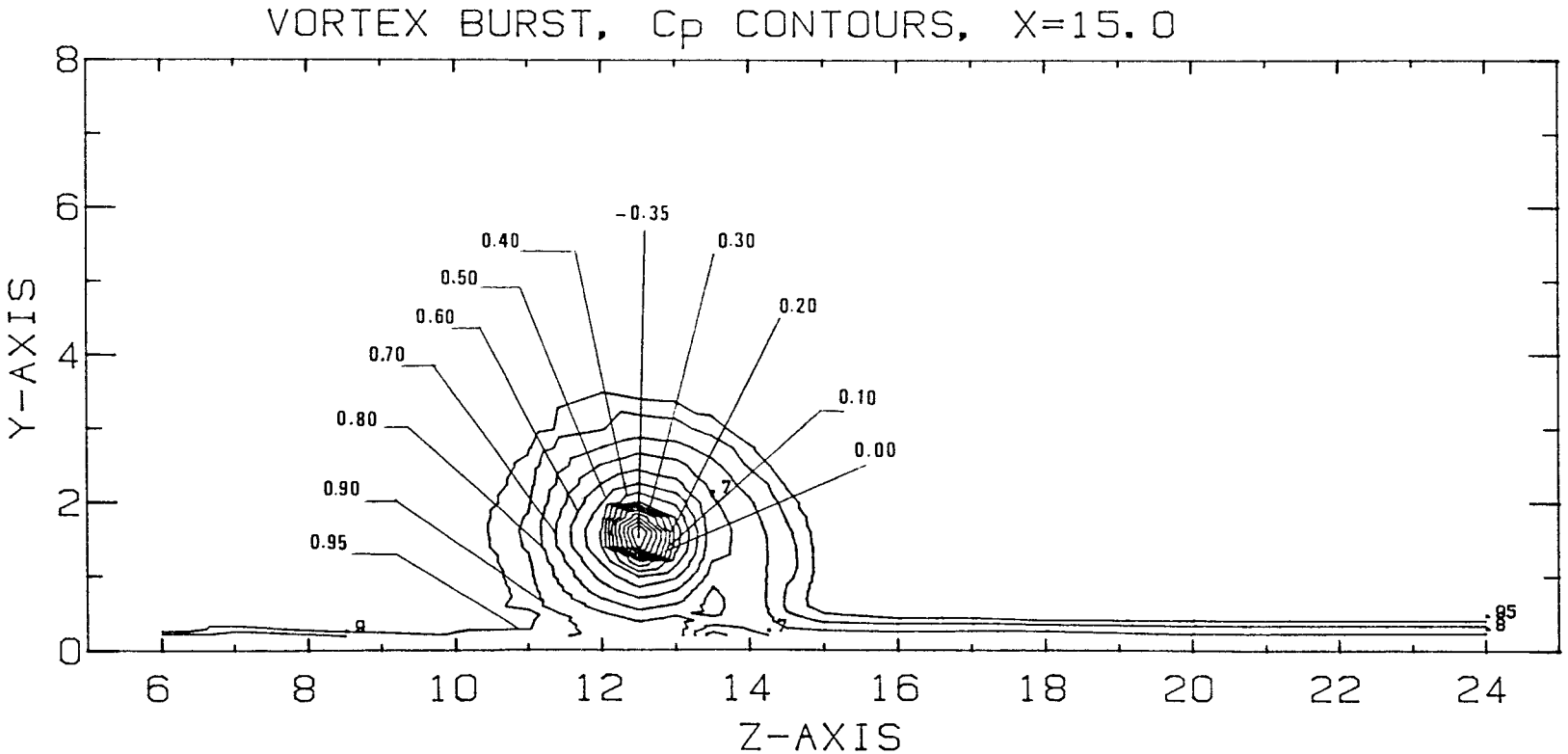

Fig. 4(b) - Total-pressure contours, configuration "C", x = 15.0".

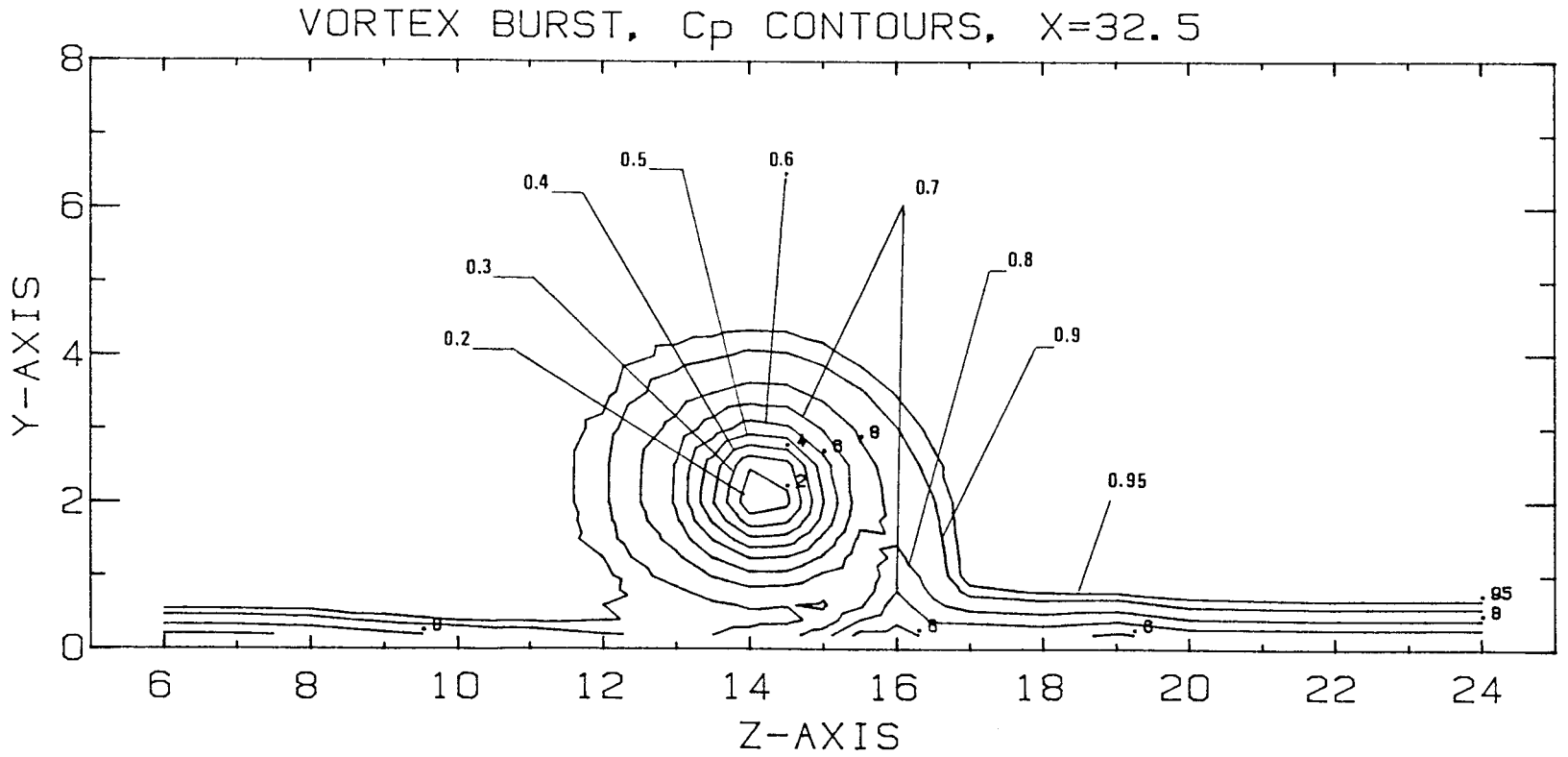

Fig. 4(c) - Total-pressure contours, configuration "C", x = 32.5".

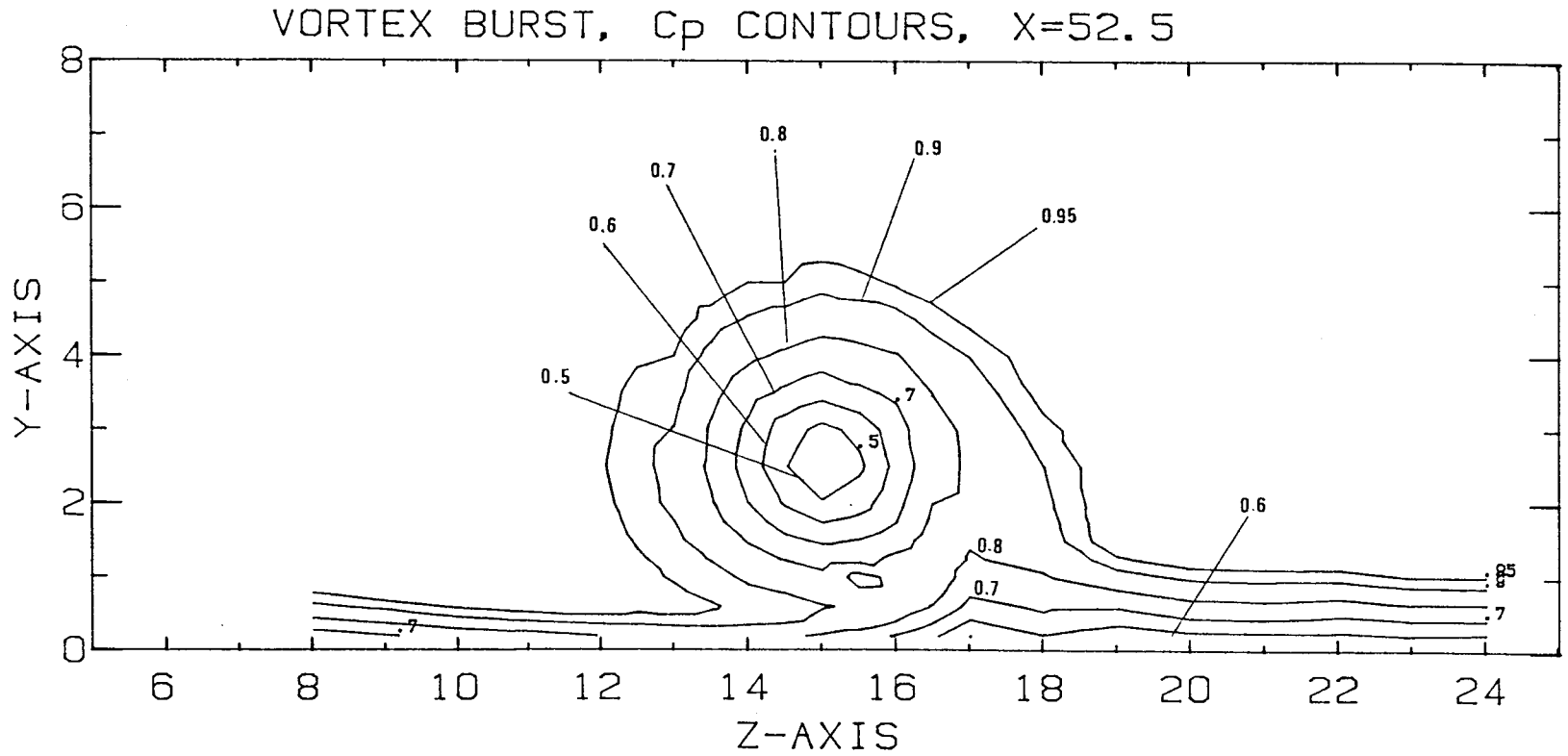

Fig. 4(d) - Total-pressure contours, configuration "C", x = 52.5".

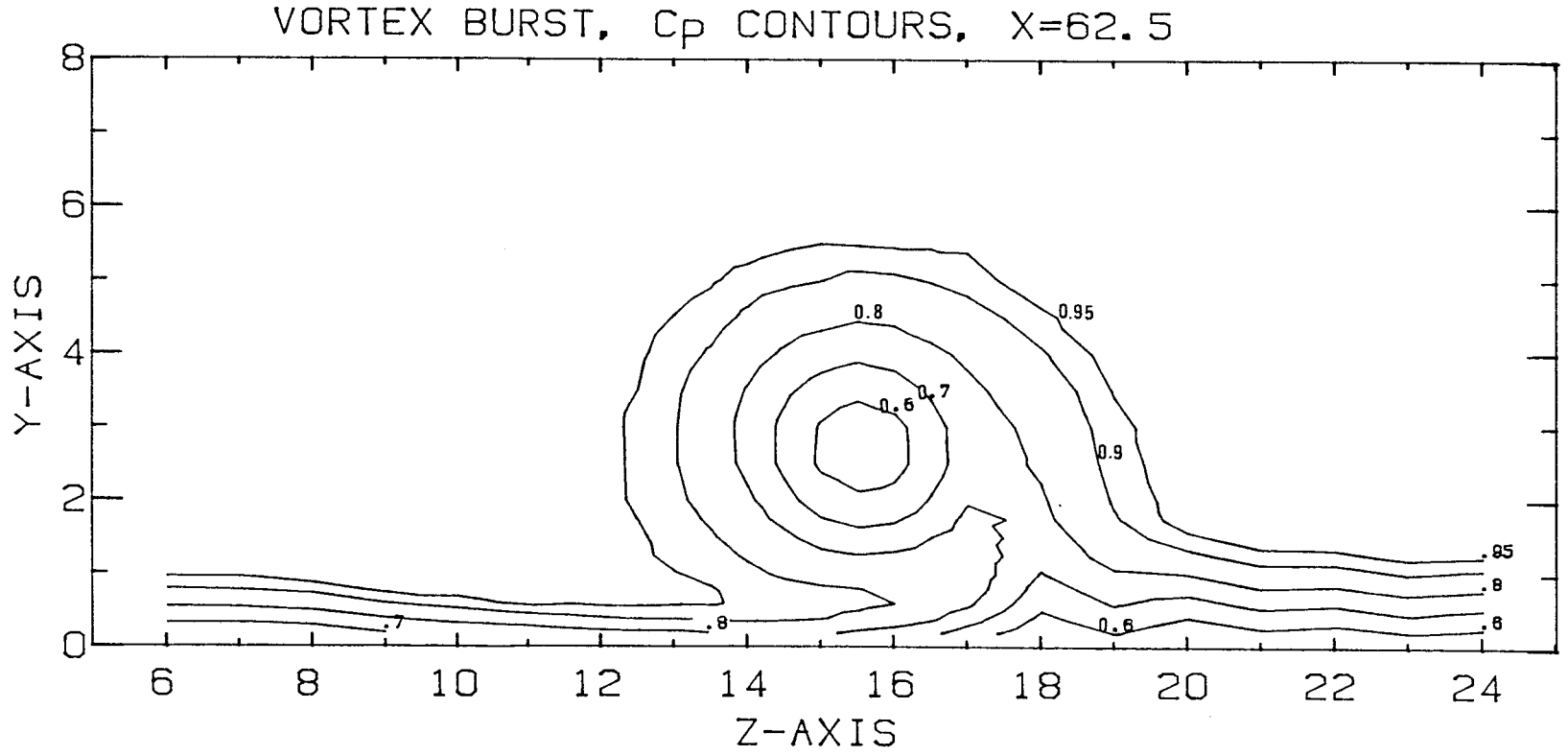

Fig. 4(e) - Total-pressure contours, configuration "C", x = 62.5".

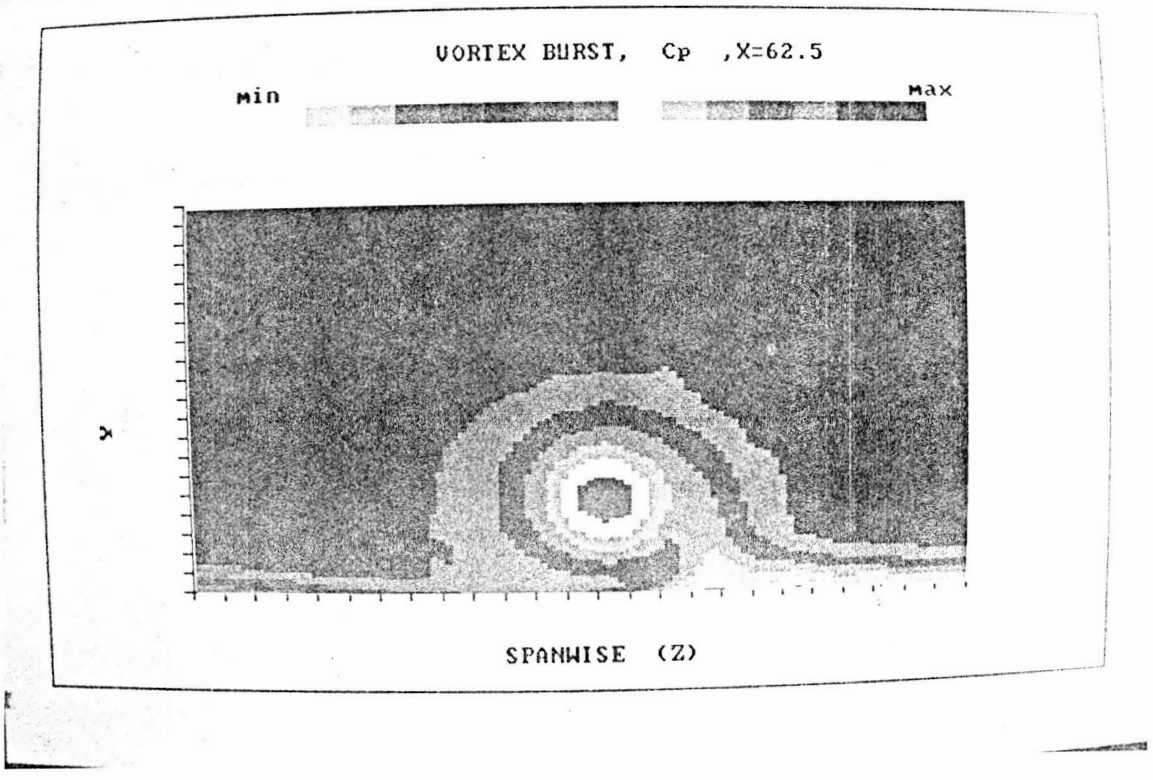

Fig. 5 - Total-pressure contours, configuration "C", x = 62.5": sample colour plot.

********Colour original********